CARPE DIEM

IN VIVO INVESTIGATION OF NEW CHITOSAN-HYDROXYAPATITE BONE SCAFFOLDS

2012

Contents

INTRODUCTION

Composites comprising calcium phosphates and natural biopolymers are widely used as biomaterials for bone tissue repair and engineering. Hydroxyapatites, Ca10 (PO4)6(OH)2, has been used as a principal inorganic component of synthetic materials for orthopedic and stomatology for a long time. This mineral can be regarded, with some limitations, as a crystallochemical analog of the main mineral constituent of human and animal skeletal tissues. A wide range of biomaterials for different clinical applications can be created on the basis of two components: nanocrystalline apatite and chitosan. Chitin is the second (after cellulose) most abundant natural polysaccharide. It forms the skeletal system of arthropod; it is also present in cell walls of fungi and bacteria. The hardness of chitin skeletal structures of arthropod is caused by the formation of natural chitin-calcium carbonate-protein complexes. Chitosan is a derivative of chitin, which can be obtained by chitin deacetylation. Chitin and chitosan are polymorphous uncrystalline or partly crystalline biopolymers. Both of them contain same monomers, N-acetyl-2-amino-2-deoxy-D-glucopyranose and 2-amino-2-deoxy-D-glucopyranose, differing in the proportion of acetylated and deacetylated monomers. Chitin and chitosan are promising materials for medical applications due to their bacteriostatic/bactericide properties, biocompatibility with human tissues, and ability to facilitate regenerative processes in wound healing. In recent years, the interest in chitosan/hydroxyapatites composite biomaterials increases significantly, which is expressed in a great number of scientific articles related to their characterization and tests. There are several ways to produce such composite materials. Most of them involve two major stages: first, the synthesis of an organic polymeric scaffold of pure or chemically treated and modified chitosan and, second, mineralization of the scaffold in simulated body fluid (the biomimetic way) or in saturated matrix solutions. The scaffolds can be made in the form of membranes, microspheres, or multilayered materials. Chitosan in such polymer substrates for mineralization can be combined with other macromolecules, such as silk fibroin or carboxymethylcellulose. Also chitin can be used as a scaffold. An inverse approach has also been described: the pre-formation of a porous hydroxyapatites scaffold with the consequent impregnation of it by chitosan. The composites obtained in such ways were characterized by different physico-chemical methods to test their potential as biomaterials,

and also a series of biocompatibility tests using cell cultures were performed, confirming biocompatibility of these composites. In addition, some researchers have reported one-step schemes of chitosan-hydroxyapatite synthesis. Yamaguchi et al. have described a one step approach, in which the composite was co-precipitated by dropping chitosan solution containing phosphoric acid into calcium hydroxide suspension. Rusu et al. have developed a stepwise co-precipitation approach using it to obtain different types of chitosan/hydroxyapatite composites with different ratios between their components. These composite materials have also been thoroughly characterized by physico-chemical techniques and have found to contain nanosized hydroxyapatite with structural features close to those of biological apatite. A further development of this approach was proposed by Chesnutt et al., they have developed microsphere-based chitosan/nanocrystalline calcium phosphate composite scaffolds. It seems that a combination of physico-chemical and structural characterization of biomaterials with their pre-clinical *in vivo* investigations is necessary to find out how the changes in structure and composition of the investigated biomaterials affect their behavior in living organisms. Since chitosan/hydroxyapatite materials could be used in bone regeneration as scaffolds in case the application of auto- or allografts is impossible for some reasons, investigation of biodegradation processes *in vivo* is important for further progress in this area (as long as an ideal scaffold material is not yet available).

AIM OF THE WORK

In the present work we have tried to synthesize, characterize and evaluate *in vivo* behavior of the simplest (uniform, made by a one-step technique) chitosan/hydroxyapatite materials as a first step towards the *in vivo* investigation of more complicated scaffold systems.

LITERATURE REVIEW

Polysaccharides are the most abundant of the four major classes of biomolecules, which also include proteins, lipids and nucleic acids. They are often classified on the basis of the sequences and linkages between their main monosaccharide components, as well as the anomeric configuration of linkages, the ring size (furanose or pyranose), the absolute configuration (D- or L-) and any other substituent present. Certain structural characteristics such as chain conformation and intermolecular associations influence the physicochemical properties of polysaccharides. For example, polysaccharides containing large numbers of hydroxyl groups are often thought of as being hydrophilic. Polysaccharides fill numerous roles in living organisms, such as the storage and transport of energy (e.g. starch and glycogen) and structural components (e.g. cellulose and chitin).

Chitin is widely distributed in nature, mainly as the structural component of the exoskeletons of crustaceans (crab, shrimp, lobster, krill, squid, crawfish and prawn) and insect cuticles, in marine diatoms and algae, as well as in some fungal cell walls. Structurally, it is an insoluble linear mucopolysaccharide consisting of *N*-acetyl-D-glucosamine (Glc*N*Ac) repeat units, linked by *β*- (1→4) glycosidic bonds. Technically, the structure of chitin is highly related to that of cellulose and may be regarded as cellulose where the hydroxyl [—OH] at the C-2 position is replaced by an acetamido [—NHCOCH3] group.

Resources of chitin for industrial processing are crustacean shells and fungal mycelia; however, its commercial production is usually associated with sea food industries, such as shrimp canning. The processing of crustacean shells mainly involves the removal of proteins (“deproteinization”; in a hot basic solution, usually sodium or potassium hydroxide), and calcium carbonate (“demineralization”; with diluted acid), both present in crustacean shells in high concentrations, encasing the chitin microfibrils.

Chitin has aroused great interest not only as an underutilized resource, but also as a new functional material of high potential in various fields. Several derivatives have been prepared from chitin, but none was as commonly studied, on both the academic and industrial level as chitosan. What probably constituted a milestone in the history of these marine polymers was the first international conference on chitin and chitosan, held in Boston, Massachusetts (U.S.A.) in 1977. It was organized by the Massachusetts Institute of Technology (MIT) Sea Grant College Program, working to promote the conservation

and sustainable development of marine resources, and to find an alternate route of exploitation of these resources of high potentials in industry; an aspect which has not been fully explored up to that point. The conference focused on several aspects of these two important natural polymers, including their recovery from the various potential sources and their applications.

Chitosan, discovered by Rouget in 1859, is a technologically important polysaccharide biopolymer. Chemically, it is a high molecular weight linear polycationic heteropolysaccharide consisting of two monosaccharide, *N*-acetyl-D-glucosamine and D-glucosamine, linked together by *β*- (1→4) glycosidic bonds (Figure 1). The relative amount of the two monosaccharide in chitosan may vary, giving samples of different degrees of deacetylation (75-95%), molecular weights (50-2,000 kDa), viscosities, pKa values, etc. Therefore, the term chitosan does not refer to a uniquely defined compound; it merely refers to a family of copolymers with various fractions of acetylated units.

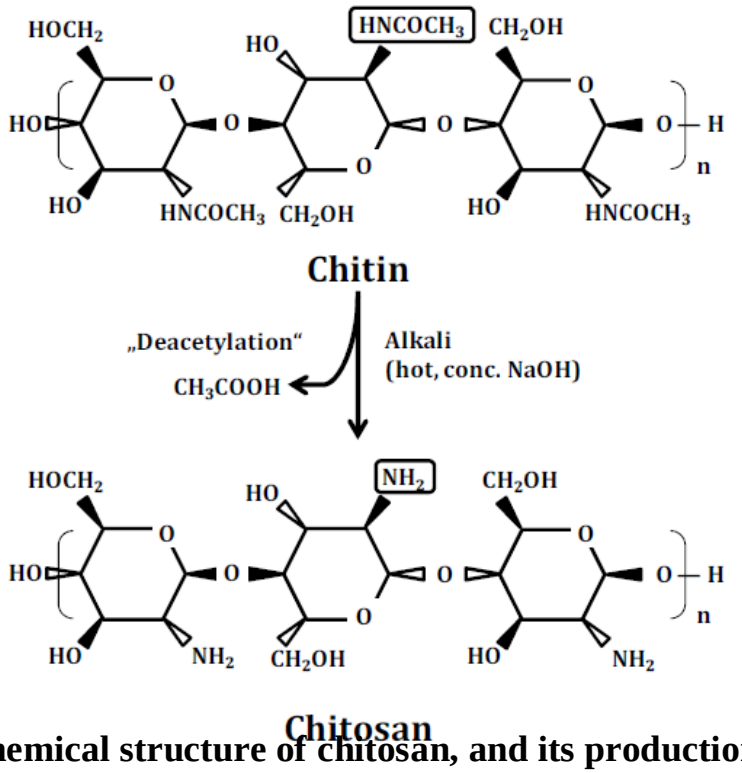

FIGURE 1: Chemical structure of chitosan, and its production from chitin.

Chitosan is primarily produced from chitin by exhaustive alkaline deacetylation: this involves boiling chitin in concentrated alkali for several hours (40–45% sodium hydroxide, 120°C, 1–3 hr). Since this *N*-deacetylation is almost never complete, chitosan is considered as a partially *N*-deacetylated derivative of chitin. Consequently, a sharp distinction between chitin and chitosan on the basis of the degree of *N*-deacetylation

cannot be drawn. Enzymatic procedures for chitin deacetylation by chitin-modifying enzymes were also investigated in the literature.

Chitosan is also found in nature, such as in cell walls of fungi of the class *Zygomycetes*, in the green algae *Chlorella* sp., yeast and protozoa as well as in insect cuticles. Recent advances in fermentation technology suggest that the cultivation of fungi (*Aspergillus niger*) can provide an alternative source of chitosan. However, chitosan from both sources differs slightly: whereas the acetyl groups in chitosan produced from crustacean chitin are uniformly distributed along the polymer chain, a chitosan of similar degree of deacetylation isolated from fungal cell walls would possess acetyl residues that are grouped into clusters.

In contrast to most of the naturally-occurring polysaccharides, e.g. cellulose, dextrin, pectin, alginic acid, agar, agarose and carragenans, which are neutral or acidic in nature, chitosan is an example of a highly basic polysaccharide. Its nitrogen content varies from 5 to 8% depending on the extent of deacetylation; it is mostly in the form of primary aliphatic amino groups.

As mentioned above, the term "chitosan" describes a heterogeneous group of polymers. Chitosan is commercially available from a number of suppliers in various grades of purity, molecular weights and molecular weight distributions, chain lengths, degrees of deacetylation, charge densities and charge distributions, salt forms, viscosities and water retention values. These properties greatly affect its physicochemical characteristics, which in turn govern almost all of its applications.

Although the underlying chemical and physical effects of some of the applications of chitosan and its derivatives are still not known in detail, considerable evidence has been gathered indicating that most of their physiological activities and functional properties depend on their molecular weight.

The molecular weight distribution of a raw chitosan preparation is influenced by variable conditions employed in the deacetylation process, such as time, temperature, concentration and nature of starting material as well as atmospheric conditions. Weight-average molecular weights of several hundreds to over one million Dalton are common, with a mean molecular mass of up to 1 MDa, corresponding to a chain length of approximately 5,000 U. Because of the influence of polymer composition and molecular weight range on the various physicochemical properties of chitosan, it is very important to

adequately characterize each batch of polymer produced. The molecular weight of chitosan can be determined by several methods, such as light scattering spectrophotometry, gel permeation chromatography and viscometry.

The main difference between chitin and chitosan lies in their solubility; deacetylation transforms the insoluble chitin into the acid-soluble chitosan. Chitosan is therefore said to be chitin that has been *N*-deacetylated to such an extent that it becomes soluble in dilute aqueous acids (e.g. 0.1 M acetic acid).

Pure, native chitosan (pKa ≅6.3) is insoluble in water, in alkaline medium and even in organic solvents. However, water-soluble salts of chitosan may be formed by neutralization with organic acids (e.g. 1-10% aqueous acetic, formic, succinic, lactic, glutamic and malic acids) or inorganic acids such as hydrochloric acid. The pH-dependent solubility of chitosan is attributed to its amino groups (—NH2), which become protonated upon dissolution at pH 6 or below to form cationic amine groups (—NH3+), increasing intermolecular electric repulsion and resulting in a polycationic soluble polysaccharide, with a large number of charged groups on a weight basis. On the other hand, chitosan tends to lose its charge at higher pH, and may therefore precipitate from solution due to deprotonation of the amine groups.

Chitosan possesses three types of reactive functional groups: an amino group at the C-2 position of each deacetylated unit, as well as primary and secondary hydroxyl-groups at the C-6 and C-3 positions, respectively, of each repeat unit. These reactive groups are readily subjected to chemical derivatization under mild conditions, to allow for the manipulation of mechanical and physicochemical properties, for example improving Chitosan’s solubility at neutral pH ranges.

Much of the commercial interest in chitosan and its derivatives during the last two decades arises from the fact that they combine several favorable biological characteristics, including biodegradability, biocompatibility and non-toxicity;properties which render natural polymers superior over present-day synthetic polymers, making them valuable materials for pharmaceutical, biomedical as well as industrial applications.

Whereas chitosan solutions are highly stable over a long period 51, there is sometimes a need for degrading chitosan to a level suitable for a particular application, or as a means of conferring solubility to chitosan at neutral pH. Several methods for producing chitosan oligomers (“chitosanolysis”) have been described in literature,

including radiation, chemical (acid hydrolysis or oxidative-reductive degradation) and enzymatic methods, of which enzymatic degradation is preferred, since reaction and thus product formation could be controlled by means of pH, temperature and reaction time.

Chitosan is susceptible to enzymatic degradation by enzymes from a variety of sources, including non-specific enzymes, such as lysozymes (present in tears, saliva, blood and milk), chitinases, cellulases or hemicellulases, proteases (papain and pronase), lipases, *ß*-1,3-1,4-glucanases, but also chitosanases. Chitosanases (chitosan *N*-acetyl-glucosamino-hydrolase) 75 have been generally recognized as enzymes that attack chitosan but not chitin, catalyzing the endohydrolysis of *ß*- (1→4) -glycosidic linkages between D-glucosamine (GlcNGlcN) residues in partly acetylated chitosan.

Over the last decade, chitosanase activities with different substrate specificities have been reported in a variety of microorganisms, including bacteria (an estimated1-7% of heterotrophic soil bacteria) and fungi as well as plants; genes encoding chitosanases have also been identified in some viruses. They have been found to belong to five glycoside hydrolase families: 5, 8, 46, 75 and 80. Interestingly, the majority of the sequenced chitosanases are produced by Gram positive microorganisms. The crystal structures of *Streptomyces* sp. N174 and *Bacillus circulans* MH-K1 chitosanases are available.

Fukamizo *et al.* proposed the classification of chitosanases into three distinct classes according to their substrate specificities: i) class I chitosanases split the Glc*N*Ac-GlcN linkage in chitosan, e.g. *Bacillus pumilus* BN262 93,193, *Penicillium islandicum* and *Streptomyces* sp. strain N174) class II chitosanases, where cleavage specificity is exclusively restricted to the GlcN-GlcN linkage, e.g. *Bacillus* sp.No.7M) class III chitosanases, which can split both GlcN-GlcN and GlcNGlc*N*Ac linkages, such as *Streptomyces griseus* HUT 6037, *Bacillus circulans* MH-K1, *Nocardia orientalis* and *Bacillus circulans* WL-12.

The low toxicity profile of chitosan compared with other natural polysaccharides is another of its many attractive features. It has been reported that the purity of chitosan influences its toxicological profile, yet its safety in terms of inertness and low or no toxicity has been demonstrated by *in vivo* toxicity studies. It's oral LD50 (median lethal dose) in mice was found to be in excess of 16 g/day/kg bodyweight, which is higher than that of sucrose. Nonetheless, it is contraindicated for people with shellfish allergy.

In their review article, Ylitalo *et al.* reported the absence of significant side effects following chitosan ingestion in human studies (for up to 12 weeks), other than mild constipation or diarrhea in a small percentage of the participants. However, Tanaka and coworkers cautioned that special care should be taken in the clinical use of chitosan over a long period of time. When chitosan was administered either orally or parenterally to mice, their body weights decreased significantly in both cases, together with disturbances in intestinal microbial flora and several histological abnormalities. Concerns have also been raised that chitosan could cause the loss of fat-soluble vitamins, decrease mineral absorption and bone mineral content and block absorption of certain medicines. No epidemiological studies or case reports investigating the association of exposure to chitosan and cancer risk in humans, no carcinogenicity studies on chitosan in animals and no *in vitro* or *in vivo* studies evaluating chitosan for mutagenic effects were identified in the available literature.

Although extensive resources were involved in both research and development of processes and applications for chitosan, only the last two decades have witnessed serious developments of a variety of technologies based on the commercial utilization of chitosan and its derivatives. Chitosan, its oligomers and a number of its derivatives emerged as new biomaterials and are currently in use or under consideration in a number of applications (pharmaceutical, cosmetic, medical, food, textile, agricultural, etc.). Due to the wide scope of applications, only a number of them will be further discussed in this section.

Introduced to the market in the 1990's, chitosan has been the subject of much research regarding its potential as a useful and promising pharmaceutical excipientin various pharmaceutical formulations. Next to the more traditional formulations, chitosan has found use in novel applications such as vaccine delivery, peptide and gene delivery, in addition to its use in tissue engineering. So far, the nasal chitosan vaccine delivery system against influenza has been tested for vaccination in human subjects, and has been proven to be both effective and protective. Chitosan's utility as a pharmaceutical ingredient gained more interest when a scientific understanding of at least some of the pharmacological activities of this versatile carbohydrate began to evolve.

In spite of the promising use of chitosan in the pharmaceutical industry, however most of the chitosan researches are directed toward medical applications. Unfortunately, a survey of the available literature revealed that there are only relatively few specific and

objective research studies to support claims, ascribing a range of rather impressive pharmacological properties to this biopolymer. Most of these studies are very difficult to take seriously, with little scientific evidence to back them up. For example, chitosan is often being heralded, and sold, as a "revolutionary" weight loss supplement, a "fat magnet", although this presumptive property is often discredited in recent studies. Given the large number of proclaimed medicinal benefits of chitosan, it comes as no surprise that the literature is filled with conflicting reports about these medical potentials.

Some studies showed that chitosan, as an immune adjuvant, could effectively promote local immune response and enhance antigen presentation. Porporatto *et al* propose the following mechanisms for the modulation of mucosal immune response: i) as a dietary fiber, chitosan might have an impact on the intestinal flora and mucosal microenvironment, thus influencing local immune function; ii) as a delivery agent, it might decrease the clearance rate and stimulate the uptake of antigens; and iii) as an adjuvant, it might provide "danger signals", being a component of fungal cell walls, possibly through the activation of components of the innate immune system such as macrophages. They therefore conclude that chitosan could be used to modulate the immune response to orally-administered antigens.

Probably one of the most prominent commercial applications of chitosan is its use as a hemostatic. Several chitosan-based wound dressings are available on the market for clinical use, including HemCon® Bandage and ChitoFlex wound dressings(HemCon Medical Technologies Inc., West Yorkshire, UK), as well as CELOX™(Medtrade Products Ltd., Crewe, England); both claimed to be FDA approved.

Chitosan is implicated as a component of host-fungal interactions. It acts as a potent elicitor of plant defense responses, activating the expression of plant defensive genes and inducing the production of pathogen-related proteins, such as chitinases and other hydrolytic enzymes. These enzymes can hydrolyze chitin and chitosan in fungal cell walls, consequently leading to growth inhibition and/or death. The induction of chitosanases and chitinases through genetic engineering has also been proposed. In addition, chitosan oligomers exhibit fungicidal properties, which make chitosan very promising as a biocontrol measure against plant pathogens. In fact, chitosan-based plant growth stimulators found their way into the market (e.g. ChitoPlant® and SilioPlant®; ChiPro

GmbH, Germany). They presumably stimulate the plant immune response against pathogens and have a growth-promoting activity.

Since a large amount of the crustacean exoskeleton is readily available as a byproduct of the seafood processing industry, the raw material for chitosan production is relatively inexpensive, and thereby the production of chitosan on a large scale from this renewable bio-resource is economically feasible. Chitosan is commercially produced in different parts of the world (Japan, North America, Poland, Italy, Russia, Norway and India) on a large scale. It has been estimated that up to109– 1010 tons of chitosan are annually produced in nature. Another important aspect to be considered is that utilizing the shellfish waste for chitin production provides a solution for the waste disposal problem, and provides an alternative for the use of this oceanic resource.

Generally Recognized as Safe (GRAS) is a designation of the FDA (Food and Drug Administration) in the United States of America, that a chemical or substance added to foods and beverages is considered safe by experts. Chitosan has not been officially proclaimed GRAS by the FDA but one Norwegian company (Primex Ingredients ASA), which manufactures shrimp-derived chitosan, has announced in 2001 that its purified chitosan product (ChitoClear®) has achieved a GRAS self affirmed status in the U.S. market. On the other hand, the FDA has approved chitosan for medical uses such as bandages and drug encapsulation. Chitosan is also widely used in foods in Italy, Finland, Korea and Japan.

The structure and composition of bone varies with the tissue site and its origin (e.g. lamellar versus cortical, intramembranous versus endochondral) as well as with age, diet, and health status. Engineering bone requires mimicking of key aspects of bone structure and composition to achieve the optimal functional tissue. To appreciate these characteristics, this chapter will review current knowledge of the functions of the mineral and matrix constituents, and how these functions have been assessed by studies of age and disease variations in tissue composition. Some comment will also be made on the current state of bone tissue engineering from the mineral and matrix points of view.

Tissue-engineered bone and other mineralized tissues will be important for the repair of lesions caused by cancer surgery, birth defects, and trauma. Since bone is unique in terms of being able to repair itself1 (e.g., fracture healing in humans and animals, limb regeneration in lower species), lessons can not only be learned by examination of these

processes, but there may be instances when tissue engineered products may only be used to enhance the natural repair process.

Bone is a composite material consisting of mineral, matrix, cells, and water. Developmentally as the cartilaginous anlage of the bone shaft is replaced by a boney matrix, that matrix is predominantly matrix (osteoid) and calcified cartilage. With age the mineral content increases, reaching a maximum value, approximated by "peak bone density," in male and female humans at different ages. In general, as the animal matures even further the total bone mineral content decreases. Diseases such as osteoporosis are associated with a decrease in total bone density, but not necessarily with decreases in the proportion of mineral in any bone, while osteomalacia is defined as a loss of bone mineral and an increase in osteoid. Conversely, osteopetrosis is an increase in both bone mineral and bone matrix, beyond that necessary for normal function.6 like many other composite materials, the integration of minerals within the organic matrix enables bone to have mechanical properties that are enhanced relative to the properties of the mineral (abrittle material) or the matrix (an elastic material) alone.

Bone has both mechanical and homeostatic functions, providing protection for the internal organs of the body and serving as a storage site and source of mineral ions. In terms of evolution, the vertebrates developed calcium phosphate skeletons, but there are lower species with other mineralized exo- and endo-skeletons that contain calcium carbonates and other phases. The compositions of those species' skeletons are reviewed elsewhere, along with discussions of how the study of these species can contribute to the development of tissue-engineered products. Bone strength is determined by the shape of the bone, the structure (arrangement of its components), that is, its geometry, and by its so-called "material" properties. The stress–strain curve of the bone has areas that have been shown to be determined predominantly by the mineral phase (elastic region) and principally by the organic phase (plastic region). The slope of the stress–strain curve is the elastic (Young's) modulus, which describes the intrinsic stiffness of the bone. Hence, all other components being equal, a more highly mineralized material will have a greater elastic modulus. The area under the stress–strain curve is the amount of energy needed to cause a fracture; thus, bones with comparable Young's module that have stress–strain curves extended into the plastic region will be more resistant to load than those that do not. There is a well-established correlation between bone mineral density (BMD) measured

radiographically and bone strength, but BMD does not completely account for bone strength.15 Rather, it is other properties of the composite tissue that are believed to explain this variation.

In the United States, there are over 500,000 bone grafts per year to replace or repair diseased or damaged bone. Autologous bone graft has long been considered the clinical "gold standard." Harvest of autograft, however, can lead to complications including chronic harvest site pain, infection, nerve damage, cosmetic deformity, and hemorrhage. In addition, autograft harvest increases operative time and cost. Allograft (e.g., cadaver bone), has been proposed as an effective alternative; yet, this material is also plagued by problems including immunogenicity, viral transmission, compromised physiologic and biomechanical properties, and potentially limited supply. Metal implants are frequently used for these purposes, but they cannot perform as efficiently as a healthy bone, and metallic structures cannot remodel with time. To help address the need for better bone substitutes, bone tissue engineers seek to create synthetic, three-dimensional bone scaffolds made from polymeric materials incorporating cells or growth factors to induce the growth of normal bone tissue.

Chapter III

MATERIALS AND METHODS

3.1 Materials preparation and characterization

The examined series consists of materials with different chitosan/apatite concentration ratios. The low molecular weight chitosan from Sigma-Aldrich (degree of deacetylation 75-85%; Brookfield viscosity 20-200 cP) was used. The substances were obtained by adding aqueous solutions of CaCl2 and NaH2PO4 (keeping Ca/P ratio equal to 1.67) into 0.2% solution of chitosan in 1% acetic acid. The necessary pH level was maintained by adding NaOH. The details of the sample preparation are listed in the Table 1. Products of the synthesis were aged, rinsed thoroughly, and then dried. Water content and chitosan-to-apatite ratio were estimated by weighing the samples before and after annealing in air at the temperature of 130 □C and 900 □C for 45 minutes.

To obtain porous materials, a lyophilization procedure was applied to wet (not dried completely) substances by using the vacuum chamber VUP-5M (SELMI, Ukraine) in which a glass sample-holder cooled with liquid nitrogen had been mounted. The frozen samples were dried under 10-3 Pa overnight.

Infrared spectra were measured on the Spectrum One spectrometer (Perkin Elmer). Before examination the powdered samples were mixed with KBr powder (2.5-3.0 mg of chitosan/apatite composite and 300 mg of KBr) and pressed into a solid disk. The Vickers hardness of the non-porous samples was measured by the standard method using the special light microscope PMT-3 (LOMO, Russia). The load of 20 grams was applied to each sample.

X-ray diffraction (XRD) crystallographic investigations were performed using the diffractometer DRON4-07 (“Burevestnik”, Russia). The Ni-filtered CuK radiation (wavelength 0.154 nm) was used with a conventional Bragg-Brentano geometry. The current and the voltage of the X-ray tube were 20 mA and 30 kV respectively. The samples were measured in the continuous registration mode (at the speed of 2 /min) within the 2-angle range from 8 to 60. All experimental data processing procedures were performed with the program package DIFWIN-1, (“Etalon PTC” Ltd.).

Scanning electron microscopy with X-ray microanalysis was performed using the electron microscope REMMA102 (SELMI, Ukraine). This instrument allows visualization of sample surface with the limit resolution of ca. 10 nm. Characteristic X-ray emission

exited by the electron probe makes it possible to estimate the elemental composition of a sample. In this work the accelerating voltage of the electron probe was set to 20 kV, the current of the probe was set to 2 nA. An energy dispersive X-ray EDX) detector was used. The analytical signal of characteristic X-ray emission was integrated by scanning the 50X50 μm2 area of sample surface.

To avoid surface charge accumulation in the electron-probe experiment, samples were covered with the thin (30-50 nm) layer of silver in the vacuum set-up VUP-5M (SELMI, Ukraine).

3.2 Animal tests

For the *in vivo* tests 48 linear laboratory rats at the age of 4 months were used. The Ukrainian National Act of animal protection against cruel treatment (Act № 3447-IV 21.02.2006) regulating the care and use of laboratory animals has been observed. At the middle one-third of right tibia of the animals perforated defects were made with a stomatological borer, diameter 2 mm, in the sterile operating room.

The width of a tibial diaphysis of adult rats is at the average form 4.2 to 4.7 mm. When a perforating bone defect is modeled, it is necessary to preserve integrity of bone, which causes the intramembranous type of bone regeneration. A model defect in this case cannot be wider than 2 mm. The 50/50 chitosan hydroxyapatites scaffolds were chosen for *in vivo* evaluation. In the experimental group of animals cylindrical ChAp rods were implanted into traumas, diameter of the rods was equal to the width of the wound channel. The control group was comprised of the rats with the analogous tibial defects, which were not filled with the investigated material. The animals were taken out of the experiment after 5, 10, 15, and 24 days after implantation. The terms of taking out corresponded to the main stages of reparative osteogenesis. The extracted bones with the defects were fixed in 10% formalin and then embedded in paraffin to prepare histological specimens. Some bones were treated with glutaraldehyde for the electron microscopy. The histological and histomorphological analyses of the extracted tissues were performed at the above mentioned stages of reparative bone regeneration.

3.3 Characterization of specimens after the *in vivo* tests

Elemental composition and morphologic characteristics of the tissues were studied by scanning electron microscopy with the X-ray microanalysis. At the same time the blood samples were taken from the caudal vein for the biochemical analysis. The levels of

calcium in serum, alkaline phosphatase and crude protein were examined. The crude protein in blood plasma was estimated by Lowry method. The calcium content in blood plasma was examined using the murexide-glycerin reagent. The alkaline phosphatase activity was determined by decomposition of phenyl phosphate with the formation of phenol and consequent reaction of the phenol with 4-aminophenazone.

To prepare histological specimens the places of defects were extracted, fixed in 10% solution of neutral formalin, decalcified in EDTA solution during two months, dehydrated in alcohol solutions with increasing alcohol concentrations, and finally embedded in paraffin. Histological microscopic sections10-12 μm thick were prepared and stained with azure-eosin and by van Giezon. The microscopic sections were then investigated using an "Olimpus" light microscope with a digital camera.

Morphometry study has been carried out using the specialized computer programs "VideoTest 5.0"and "VideoSize 5.0" (St. Petersburg, Russia). 3 days after the defects were made, the cellular composition of regenerated tissue was investigated, i.e. the percentage of certain cell populations compared with the total amount of cells in the place of a defect. The number of fibroblasts, macrophages, lymphocytes, plasmocytes, neutrophils, and undifferentiated cells was calculated. Cells in the samples were counted under 1000x magnification, which allows to determine the phenotypic peculiarities of different cellular populations. Poorly differentiated bone marrow cells and undifferentiated connective tissue cellular elements were defined as undifferentiated cells. The cells had been counted over the whole section of a model defect. The number of macrophages, lymphocytes, fibroblasts, plasmocytes, and undifferentiated cells is given as percentage to the total number of cells in the defect. In histological specimens of the next stages of reparative osteogenesis the percentage of granulation, fibroreticular, and membranes reticulated splenial bone tissues as well as of red bone marrow were determined.

CHAPTER IV

RESULTS AND DISCUSSION

The preparation conditions for series of ChAp composites and their chitosan-to-apatite ratio estimated by simple thermogravimetric analysis are listed in the Table 1. The water content was estimated from the weight loss after heating the samples at 130ºC. The total mineral (calcium phosphate) content was measured as a sample weight after complete burnout of organic moiety at 900ºC. Here we assumed that the weight loss at 130 °C corresponds to the water fraction and the weight loss at 900°C corresponds to the polysaccharide fraction. As it is seen, the experimental data are in reasonable agreement with the declared chitosan-to-apatite ratio.

Table 1

Chitosan-to-apatite ratio of samples estimated from thermogravimetric measurements. In each case 1000 ml of0.2 wt% chitosan solution was used for Ch/Ap preparation.

No	Ch/Ap preparation			Data of thermogravimetric analysis		
	Ch/Ap composites, (specified weight ratio)	mineral solution		percentage of components determined from the weight loss		
		$CaCl_2$ 1M, ml	NaH_2PO_4 1M, ml	H_2O, wt%	chitosan, wt%	apatite, wt%
1	ChAp 15/85	113.3	68.0	9.0±1.2	14.9±3.09	76.1±3.09
2	ChAp 30/70	46.6	28.0	11.4±0.2	25.4±0.60	63.2±0.60
3	ChAp 50/50	20.0	12.0	3.3±1.0	49.3±2.2	47.4±2.2
4	ChAp 80/20	5.0	3.0	8.9±1.0	73.0±2.0	18.1±2.1

From IR spectroscopy studies of ChAp series with different proportions between components we can conclude that the major absorbance bands of IR spectra correspond to hydroxyapatites, though their width increases significantly and the bands characteristic to chitosan appear as the chitosan content increases (Fig. 1). The bands at 1000-1100 cm-1 and 500-600 cm-1 correspond to different modes of PO4 group in hydroxyapatites. Broadening of the band at 1050 cm-1 reflects the presence of polymer and its interaction with phosphate groups. The bands at 1420-1485 cm-1 and at ~875 cm-1 are derived from carbonate ions in apatite. The phosphate stretching vibration bands from hydroxyapatite were indicated at 1000-1100 cm-1 whereas the phosphate bending vibration bands situated at 500-600 cm-1. The strongest characteristic CO3 bands at 1420-1485 cm-1 are also visible. The bands at 1550-1700 cm-1 can be attributed to superposition of hydroxyapatite OH group and chitosan amide I and amide II. The bands at 3600-3700 cm-1 can be

assigned to hydroxyl groups present in the structure of chitosan, the bands at 2800-2950 cm-1 belong most probably to C-H stretch.

Fig. 1

IR spectra of hydroxyapatites and chitosan/hydroxyapatites scaffolds with different chitosan/hydroxyapatites ratio.

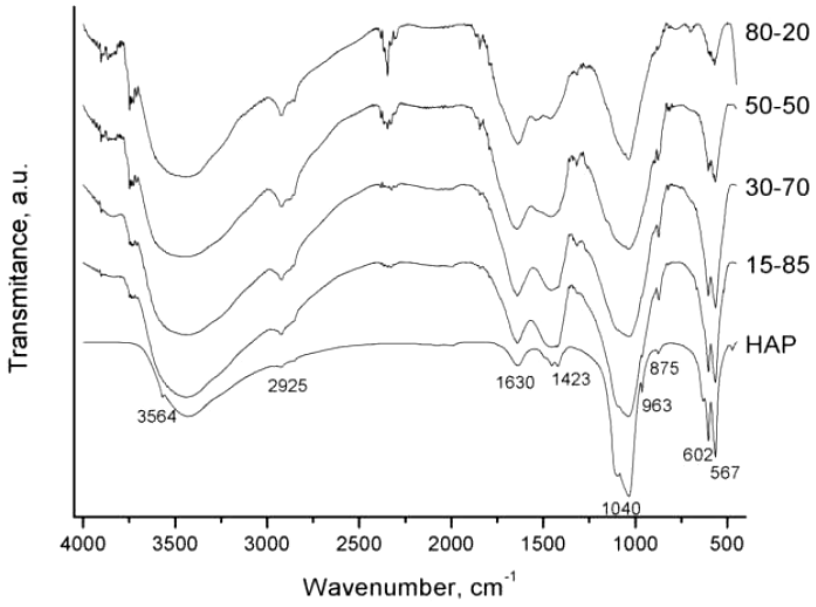

XRD patterns suggest the presence of nanocrystalline apatite, its crystallinity decreases as content of chitosan increases **(Fig. 2)**.

Fig. 2

X-ray diffraction patterns of ChAp samples with different initial component ratio

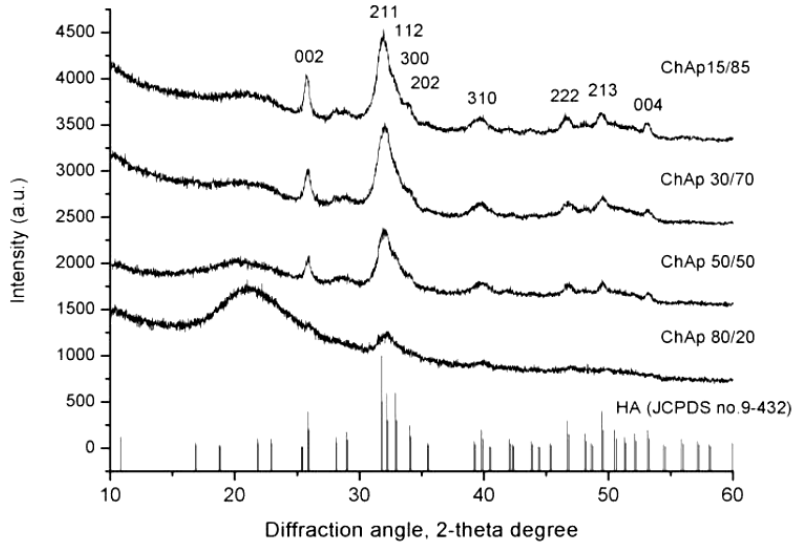

As it follows from the diffraction peak broadening, which is inversely proportional to the crystallite size, the more chitosan is present in the composite, the less is the average size of apatite crystals. The semi quantative evaluation of the crystallite size were

performed by the analysis of (002) line profile in the same way as in the work. Shortly, at the negligible lattice microstrain, the crystallite size was determined from the physical broadening of the (002) line from Scherrer's formula:

$$L = \frac{K\lambda}{\beta \cdot \cos\vartheta},$$

Where β is the line breadth of the pure diffraction profile resulting from small crystallite size, and K is a constant approximately equal to unity and related to crystallite shape. Powdered polycrystalline NaCl was used as reference material free of size and microstrain broadening. The result of estimation suggests that for chitosan/apatite ratio equal to 50/50, the size of apatite crystallites in the composite is ~20 nm, which is comparable with the crystallite size of bioapatite in bone tissue. The average size of bone apatite is normally ~20 nm, which was proved by different experimental techniques.

Slightly increased intensity of the (002) and (004) peaks compared with the reference data suggests that the apatite crystallites are elongated along the crystallographic axis c (what is also characteristic for bioapatite of bone tissue). The XRD analysis in combination with IR spectroscopy studies clearly indicated the formation of chitosan/hydroxyapatites composites.

The Vickers hardness of non-porous ChAp composites is shown in the Table 2. These data indicate the decrease of material strength with the increase of chitosan percentage and are in reasonable agreement with the value of 0.396 GPa recently reported for the cortical bone.

Table 2

The Vickers hardness of the samples with different chitosan-to-apatite ratio.

No	Ch/Ap composites, (specified weight ratio)	Vickers hardness, GPa
1	ChAp 15/85	0.22
2	ChAp 30/70	0.15
3	ChAp 50/50	0.12
4	ChAp 80/20	0.14

The porous composite materials are much less hard than the solid ones; their measured hardness values were too much spread to be conclusive; it was difficult to measure the dent size because of the complicated profile of sample surface.

Ca/P ratio in the ChAp samples measured by scanning electron microscopy with EDX microanalysis was close to that of apatite (1.67). The EDX spectra of the ChAp samples did not show any pronounced peaks of Na and Cl (Fig. 3), which suggested that the synthesized apatite did not have substitutions in the cation (Na → Ca) and anion (Cl → OH) sublattices at the level detectable by the technique. In lyophilized materials a network of micrometer and submicrometer pores has been observed. The porous materials were produced by lyophilization of the samples immediately after rinsing and ageing. In the microscopic images of these materials two systems of pores can be visually distinguished (Fig. 4). Statistical treatment using the specialized computer programs "VideoTest 5.0" and "VideoSize 5.0" (St. Petersburg, Russia) has shown that the "small" pores have the average diameter of 30 μm, the "big" ones of 50 μm. Such pores could promote the bone tissue ingrowths into implanted material.

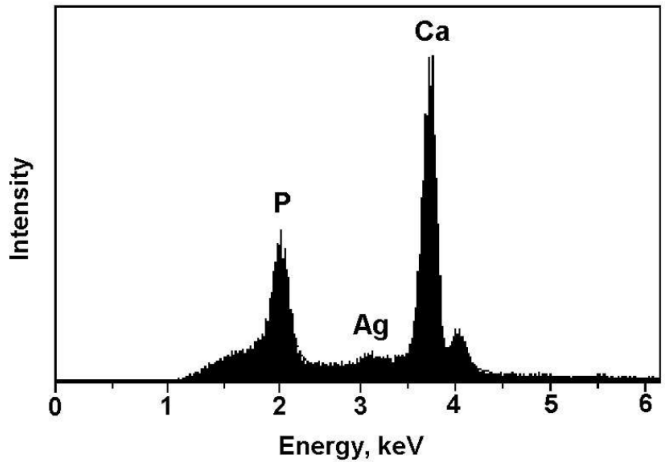

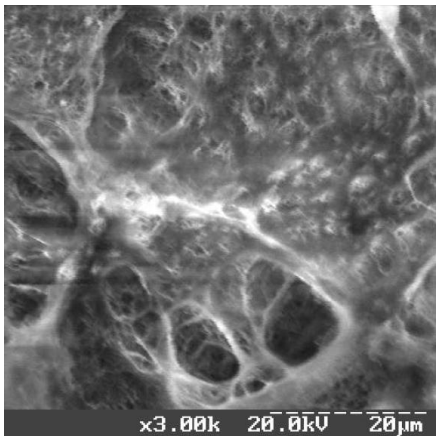

Fig. 3 EDX spectrum of ChAp 50/50 composite.	Fig. 4 Microstructure of porous ChAp.

The content of Ca and P (measured by EDX microanalysis) in bones of the model animals after implantation of solid ChAp biomaterial with the 50/50 component ratio is shown in the Fig. 5. In this case it is clearly seen that in the presence of implanted ChAp, the Ca and P concentrations in bone tissue near the defect were restored much faster than in the control group (where the bone defects were not filled with implants).

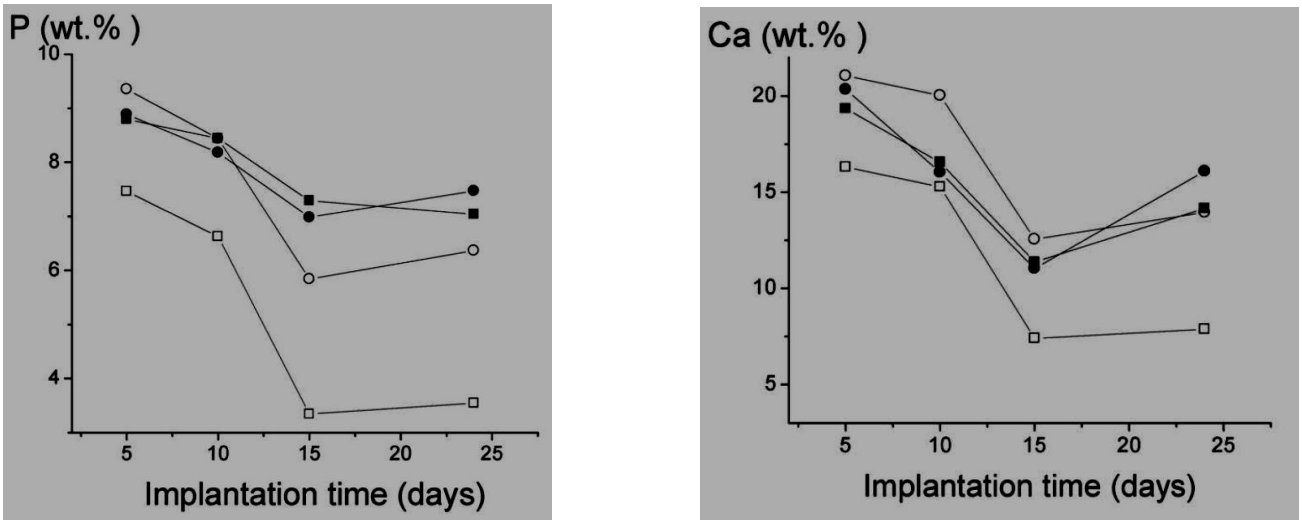

Fig. 5 The content of Ca and P in bone tissue near the site of implantation (squares) and at the distance of 15 mm (circles) vs. implantation time. Non-filled symbols correspond to the control experiment: the defect without an implant.

The biochemical blood values for the experimental and control groups of animals are given in the Table 3. The protein and alkaline phosphatase level in the blood of experimental animals do not differ from that of the control group. The comparison of the values with the results of microanalysis of bones with implanted ChAp indicates that calcium mobilization from the surface of intact tissues decreases while its content in blood plasma comes to normal. Low Ca mobilization from neighboring bones can decrease the bone strength loss accompanying the regenerative processes. As it is proved in numerous works, the bone strength depends strongly on the mineral content, i.e. Ca and P concentration.

Table 3

Biochemical blood values of the experimental and control groups of animals.

Value	10 days		15 days		24 days	
	control	experimental	control	experimental	control	experimental
Protein, g/L	52.94±1,78	64.05±2.86	51.11±2.04	60.35±1.88	63.79±2.41	61.22±2.66
Alkaline phosphatase, nmol/sL	3116.91±192.58	2401.63±145.27	2334.01±471.20	2774.02±266.52	2343.42±207.77	4236.53±523.31
Ca, mmol/L	2.84±0.33	2.06±0.60	2.28±0.14	1.48±0.24	2.58±0.27	2.05±0.49

These data suggest that nano-sized apatite crystals incorporated into chitosan matrix, being implanted *in vivo*, participate immediately in reparative biochemical processes of living bone tissue. Apparently, these are Ca and P from the apatite crystals of implanted

material that are used for the regenerated bone formation. This decreases mobilization of these elements from the bone tissue near a defect.

The porous materials have shown osteoconductive properties in the *in vivo* tests. In 3 days after implantation, pores of ChAp were filled with the cells of leukocyte-macrophage and fibroblastic differons, which was the evidence of progress in osteoreparative process. Further, the formation of fibro reticular and membrane reticulated primary bone tissue trabecules occurred with their subsequent calcification and remodeling into lamellar bone tissue. Starting from the 10th day, the integration of ChAp into newly formed tissue was observed, and by the 24th day the replacement of the implant by the young bone took place. The above-described dynamics is specific only for porous samples of ChAp. Solid (nonporous) implants did not improve histological pattern of the reparative process.

The osteoconductive properties of a ChAp composite material can be observed after implantation of it into the bone defect at the first stages of regenerated bone tissue development. In the Fig. 6 there are clearly visible pores filled with the typical for such regeneration stages cell and tissue species.

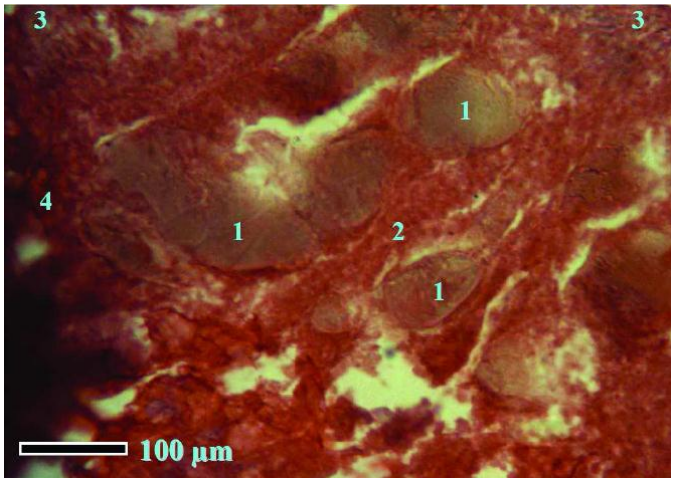

Fig. 6 Area of the tibial defect, 5 days after traumatization:

1. ChAp.
2. Pore with posttraumatic hematoma cells.
3. Granulation tissue.
4. Capillary.

Young granulation tissue (GT) dominates in the regenerate, its content is 25.25±5.14%. We did not however observe the close connection of tissue components with the material of the implant, which can be explained by the early stage of observations and high rate of granulation tissue formation. GT occupies the peripheral segments of the defect (which is similar to the patterns of the control animals). The central pores of the implant are filled mostly with the cells of posttraumatic hematoma. The normal cell

composition plays an important role in new bone formation. At the initial stage of regeneration the neutrophils secrete cytokines regulating proliferation, cell differentiation, and phagocytosis. The lymphocytes and plasmocytes are able to regulate angiogenesis and fibroblast migration. Also they have stimulating influence on macrophages. The macrophages in their turn act as regulators of inflammatory processes; they have chemotactic action on fibroblasts and provide intercellular cooperation in the focus of trauma. Fibroblasts are the cells which actively produce collagen beginning from the first days after trauma providing the formation of a soft natural scaffold. So, proliferation and differentiation of cells at the first stage of the reparative regeneration is crucial for the formation of the critical mass of cells, which is important for the formation of tissue structures in trauma site at the following stages of regeneration. In one field of view different cell phenotypes were observed: young secreting cells, mature macrophages filled with detritus, dying cells. The cell percentage for the experimental and control groups of animals are given in the Table 4. In the inner pores the edges of the material were blurred which could be indicative of the beginning of ChAp osteointegration and high activity of cells in this site of the defect. Both in the peripheral and in the central pores vascular invasion was observed, mostly of the sinusoidal type. The vessels were surrounded by a layer of perivascular cells and secreting fibroblasts, which were more numerous in peripheral sections.

In 10 days after introduction of the implant its intense biodegradation takes place with the formation of tissue-specific structures of regenerate. The intense growth of fibroreticular tissue (FT) with more ordered fiber arrangement can be observed in the area of the defect, and also formation of bone trabeculae of membrane reticulated bone begins (Fig. 7). FT is situated mostly along the periphery of the defect, while its central areas are filled with remains of granulation tissue with the great number of fibroblasts, macrophages and sinusoidal capillaries. For the first time the formation of membrane reticulated bone tissue is observed which can be the evidence of the osteoblastic type of reparative processes. The amount of new bone tissue is approximately the same as in the case of the control animals (34.58±9.27%), so the implant cannot be regarded as osteoconductive. At the same time, the integration and close interconnection of the forming bone trabeculae and ChAp can be observed.

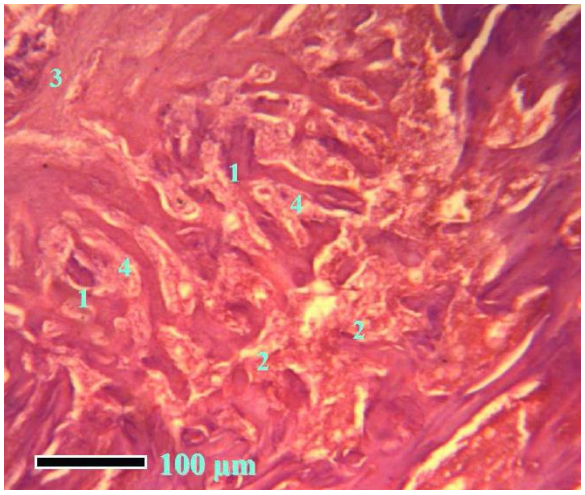

Fig. 7 Area of the tibial defect, 10 days after traumatization:

1. ChAp.
2. Granulation tissue.
3. Fibroreticular tissue.
4. Bone trabeculae.

The histological pattern of the regenerate on the 15th day is similar to that of the 10th day (Fig. 8).Both fibroreticular and bone tissues were present; the bone tissue had formed a denser network of trabeculae than in the previous observation time. Granulation tissue was completely absent. The active remodeling of membrane reticulated bone into splenial bone and its mineralization takes place, which is indicated by the increase of staining intensity of the bone trabeculae.

.

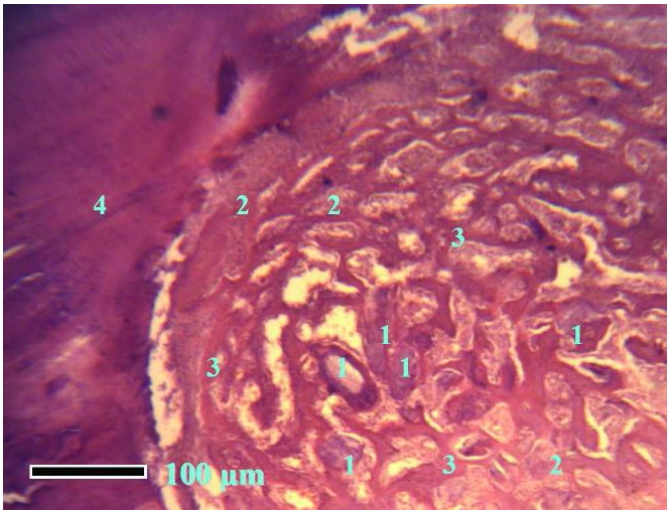

Fig. 8 Area of the tibial defect, 15 days after traumatization:

1. ChAp.
2. Fibroreticular tissue.
3. Bone trabeculae.
4. “Parent” bone.

The percentage of FT, membrane reticulated bone and splenial bone is correspondingly 28.43±7.97%, 40.21±9.65% and 10.87±3.22%, which is in agreement with the control series of animals. The remains of the implant are situated mainly in the centre of the defect, connected closely with the forming bone trabeculae and stained non uniformly, which suggests their integration into the newly formed bone matrix.

On the 24th day of observation bone tissue occupies most of the area of the defect (Fig. 9). The deeper parts of the regenerate are formed with membrane reticulated bone tissue with stainability close to that of the "parent" bone. The number of osteoblasts on the surface of trabeculae decreases, which indicates that intense bone matrix formation processes stops, and remodeling processes begin.

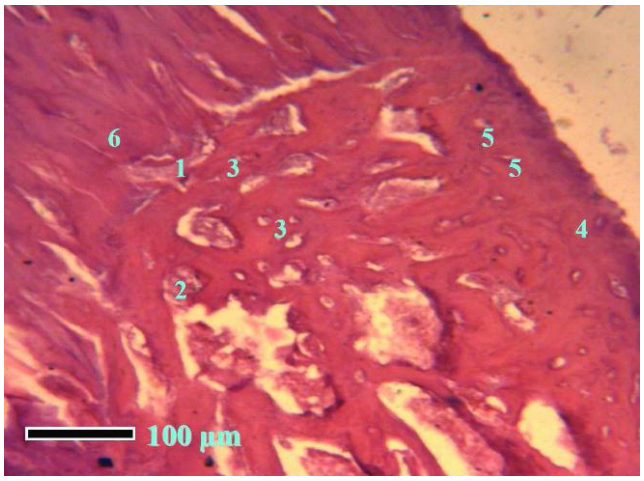

Fig. 9 Area of the tibial defect, 24 days after traumatization:

1. ChAp
2. Fibroreticular tissue.
3. Membrane reticulated bone tissue.
4. Splenial bone tissue.
5. Osteon.
6. "Parent" bone.

The remains of not degraded ChAp are pushed off to the periphery and are on the boundary of the "parent" bone. The tight bonding of the implant with newly formed bone matrix is observed; the bonding with the "parent" bone is less tight. The cortical plate in the place of the defect is formed mostly by the splenial bone in which intensive remodeling processes are observed, this is indicated by the presence of both secondary and primary osteons. The primary ones at this observation stage are much more numerous. So it is safe to say that the completion of the primary formation of neogenic bone and the beginning of remodeling processes. The implant's remains are closely integrated into the newly formed matrix and are subject to biodegradation in the course of bone remodeling.

CONCLUSIONS

1. A series of chitosan/hydroxyapatites composite materials has been synthesized in aqueous medium from chitosan solution and soluble precursor salts by a one step co-precipitation method.

2. XRD patterns of the materials suggest the presence of nanocrystalline apatite with the average crystallite size of approximately 20 nm. The similar size of crystallites is characteristic for natural bone bioapatite.

3. The results of IR spectroscopy studies suggest the presence of carbonate ions in the synthesized materials. Thus, this relatively simple synthesis procedure allows to obtain composite materials with nanocrystalline carbonate-substituted hydroxyapatites similar to natural bone bioapatite.

4. Histomorphological studies have shown that the porous chitosan/hydroxyapatites materials undergo almost complete biodegradation. The complete replacement of porous chitosan/hydroxyapatites composite implant by newly formed bone tissue within bone defects in rats takes place on the 24th day of implantation.

5. The results of the present study suggest the high potential of simple chitosan/hydroxyapatites composite scaffolds produced by the one-step co-precipitation method as a filling material for orthopedic and stomatology.

REFERENCES

1. Wahl DA, Czernuszka JT. Collagen-hydroxyapatite composites for hard tissue repair. European Cells and Materials 2006; 11: 43-56.

2. Chang MC, Ko CC, Douglas WH. Preparation of hydroxyapatite-gelatin nanocomposite. Biomaterials 2003; 24: 2853-2862.

3. Yamaguchi I, Tokuchi K, Fukuzaki H, Koyama Y, Takakuda K, Monma H, Tanaka J. Preparation and microstructure analysis of chitosan/hydroxyapatite nanocomposites. J BiomedMater Res 2001; 55: P. 20-27.

4. Rusu VM, Chuen-How Ng, Wilke M, Tiersch B, Fratzl P, Peter MG. Size-controlled hydroxyapatite nanoparticles as self-organized organic–inorganic composite materials. Biomaterials 2005; 26: 5414 –5426.

5. Hu Q, Li B, Wang M, Shen J. Preparation and characterization of biodegradable chitosan/hydroxyapatite nanocomposite rods via in situ hybridization: a potential material as internal fixation of bone fracture. Biomaterials 2004; 25: 779-785.

6. Elliott JC. Calcium Phosphate. Biominerals. In: Kohn MJ, Rakovan J, Hughes JM, editors. Phosphates: geochemical, geobiological and materials importance. Series: Reviews in mineralogy and geochemistry, vol. 48. Mineralogical Society of America, Washington, DC:2002. p. 427–454.

7. Zhang Y, Zhang MQ. Synthesis and characterization of macro-porous chitosan/calcium phosphate composite scaffolds for tissue engineering. J Biomed Mater Res 2001; 55: 304-312.

8. Oliveira JM, Rodrigues MT, Silva SS, Malafaya PB, Gomes ME, Viegas CA, Dias IR, Azevedo JT, Mano JF, Reis RL. Novel hydroxyapatite/chitosan bilayered scaffold for osteochondral tissue-engineering applications: Scaffold design and its performance when seeded with goat bone marrow stromal cells. Biomaterials 2006; 27: 6123 –6137.

9. Zhao F, Grayson WL, Ma T, Bunnell B, Lu WW. Effects of hydroxyapatite in 3-D chitosan–gelatin polymer network on human mesenchymal stem cell construct development. Biomaterials 2006; 27: 1859 –1867.

10. Li J, Chen YP, Yin Y, Yao F, Yao K. Modulation of nano-hydroxyapatite size via formation on chitosan–gelatin network film in situ. Biomaterials 2007; 28: 781 –790.

11. Wang L, Li C. Preparation and physicochemical properties of a novel hydroxyapatite/chitosan – silk fibroin composite. Carbohydrate Polymers 2007; 68: 740 – 74.

12. Jiang LY, Lia YB, Zhanga L, Wang XJ. Preparation and characterization of a novel composite containing carboxymethyl cellulose used for bone repair. Materials Science and Engineering C 2009; 29: 193-198.

13. Madhumathi K, Binulal NS, Nagahama H, Tamura H, Shalumon KT, Selvamurugan N, Nair SV, Jayakumar R. Preparation and characterization of novel β-chitin–hydroxyapatite composite membranes for tissue engineering applications. International Journal of Biological Macromolecules 2009; 44: 1-5.

14. Jiang L, Li Y, Wang X, Zhang L, Wen J, Gong M. Preparation and properties of nanohydroxyapatite/chitosan/carboxymethyl cellulose composite scaffold. Carbohydrate Polymers 2008; 74: 680–684.

15. Li J, Dou Y, Yang J, Yin Y, Zhang H, Yao F, Wang V, Yao K. Surface characterization and biocompatibility of micro- and nano-hydroxyapatite/chitosan-gelatin network films. Materials Science and Engineering: C. 2008; 29, 4: 1207-1215.

16. Aimoli CG, Beppu MM. Precipitation of calcium phosphate and calcium carbonate induced over chitosan membranes: A quick method to evaluate the influence of polymeric matrices in heterogeneous calcification. Colloids and Surfaces B: Biointerfaces 2006; 53: 15–22.

17. Muzzarelli RAA. Chitins and chitosans for the repair of wounded skin, nerve, cartilage and bone. Carbohydrate Polymers 2009; 76: 167-182.

18. Kong L, Gao Y, Lu G, Gong Y, Zhao N, Zhang X. A study on the bioactivity of chitosan/nanohydroxyapatite composite scaffolds for bone tissue engineering. European Polymer Journal 2006; 42: 3171 –3179.

19. Leonor IB, Baran ET, Kawashita M, Reis RL, Kokubo T, Nakamura T. Growth of a bonelike apatite on chitosan microparticles after a calcium silicate treatment. Acta Biomaterialia 2008; 4:1349 –1359.

20. Manjubala I, Scheler S, Bossert J, Jandt KD. Mineralisation of chitosan scaffolds with nanoapatite formation by double diffusion technique. Acta Biomaterialia 2006; 2: 75 –84.

21. Ito M. *In vitro* properties of a chitosan-bonded hydroxyapatite bone-filling paste. Biomaterials1991; 12: 41-45.

22. Ge Z, Baguenard S, Lim LY et al. Hydroxyapatite-chitin materials as potential tissue engineered bone substitutes. Biomaterials 2004; 25: 1049-1058.
23. Korzh NA, Dedukh NV. Reparative regeneration of bone: modern view of the problem. Regeneration stages. Orthopaedy, traumatology, and prosthetics (Ortopedia, travmatologia i protezirovanie) 2006; 1: 77–83 (in Russian).
24. Wheater PR, Burkitt HG. Functional Histology. 2nd ed. 1987.
25. Danilchenko SN, Kukharenko OG, Moseke C et al. Determination of the bone mineral crystallite size and lattice strain from diffraction line broadening. Cryst Res Technol 2002; 37, 11: 1234– 1240.
26. Chesnutt BM, Viano AM, Yuan Y, Yang Y, Guda T, Appleford MR, Ong JL, Haggard WO, Bumgardner JD. Design and characterization of a novel chitosan/nanocrystalline calcium phosphate composite scaffold for bone regeneration. Journal of Biomedical Materials ResearchPart A 2009; 88, 2: 491-502.
27. Abdel-Fattah WI, Jiang T, El-Tabie El-Bassyouni G, Laurencin CT. Synthesis, characterization of chitosans and fabrication of sintered chitosan microsphere matrices for bone tissue engineering. Acta Biomaterialia 2007; 3: 503 –514.
28. Danilchenko SN, Koropov AV, Protsenko IYu, Sulkio-Cleff B, Sukhodub LF. Thermal behavior of biogenic apatite crystals in bone: An X-ray diffraction study. Cryst. Res. Technol. 2006; 41,3: 268-275.
29. Klug HP, Alexander LE. X-ray diffraction procedures for polycrystallite and amorphous materials, 2nd edition. John Wiley and Sons, New York, 1974.
30. Pramanik S, Agarwal AK, Rai KN. Trends Biomater. Artif. Organs. 2005; 19: 46-53.
31. Tai K, Qi HJ, Ortiz C. Effect of mineral content on the nanoindentation properties and nanoscale deformation mechanisms of bovine cortical bone. Journal of material science: materials in medicine. 2005; 16: 947-959.
32. Van der Linden JC, Birkenhäger-Frenkel DH, Verhaar JAN, Weinans H. Trabecular bone's mechanical properties and affected by its non-uniform mineral distribution. Journal of Biomechanics. 2001; 34, 12: 1573-1580.
33. Boivina G, Balaa Y, Doubliera A et al. The role of mineralization and organic matrix in the icrohardness of bone tissue from controls and osteoporotic patients. Bone. 2008; 43: 532 - 538.
34. Stephen CC. Bone mechanics handbook Informa Health Care. 2001; 980 p.

35. Eppell SJ, Tong W, Katz JL, Kuhn L, Glimcher MJ. Shape and size of isolated bone mineralites measured using atomic force microscopy. Journal of orthopaedic research. 2001; 19: 1027-1034.

36. Cancedda R, Quarto R, Giannoni P et al. Cell therapy and bone repair. Eur. Cells Mater. 2003; 5,Suppl. 2: 2-3.

37. Kaspar D, Neidlinger-Wilke C, Holbein O. Mitogens are increased in the systemic circulation during bone callus healing. J. Orthop. Res. 2003; 21, 2: 320-325.

38. Ross FP. Cytokine regulation of osteoclast formation and function. J. Musculoskel. Neuron.Interact. 2003; 3(4): 282–286.

39. Grundnes O, Reikeras O. The importance of the hematoma for fracture healing in rats. ActaOrthop. Scand. 1993; 64, 3:340-342.

40. Balázsi C, Bishop A, Yang JHC, Balázsi K, Wéber F, Gouma PI. Biopolymer-hydroxyapatite scaffolds for advanced prosthetics. Composite Interfaces. 2009; 16: 191-200.

41. Dyer JR. Applications of absorption spectroscopy of organic compounds. 1965; Prentice-Hall inEnglewood Cliffs, N.J.:143 pp.

42. Kumirska J, Czerwicka M, Kaczyński Z, Bychowska A, Brzozowski K, Thöming J, StepnowskiP. Application of spectroscopic methods for structural analysis of chitin and chitosan. MarineDrugs. 2010; 8: 1567-1636.

43. Fowler BO. Infrared studies of apatites. I. Vibrational assignments for calcium, strontium, and barium hydroxyapatites utilizing isotopic substitution. Inorg. Chem. 1974; 13 (1): 194–207.

44. Markovic M, Fowler BO, Tung MS. Preparation and comprehensive characterization of a calcium hydroxyapatite reference material. J. Res. Natl. Inst. Stand. Technol. 2004; 109: 553-568.